

# Sorption Paper Title

Jonathan G. V. Ström<sup>a</sup>, Shuai Xie<sup>a</sup>, Eric M. Suuberg<sup>a</sup>

*These authors contributed equally to this work*

<sup>a</sup>*Brown University, School of Engineering, Providence, RI, USA*

---

## Abstract

Abstract here

*Keywords:* Vapor intrusion, Temporal variability, Sorption, Attenuation factor

---

## 1. Introduction

Many vapor intrusion (VI) contaminants has the capacity to sorb onto soil and various common indoor materials, but the role and more importantly - the consequences of these sorption processes in VI are poorly understood[1, 2? ]. The migration of contaminant vapors from its source into the affected building and potential indoor sources are usually the prime concern in VI investigations. Rarely is the sorbed contaminant vapors in the soil or indoor considered in an investigation, but these may potentially act as a capacitor, storing and releasing contaminant vapors in response to a change in contaminant concentration. Consequently, contaminant vapors may be much more persistent at a site that has undergone remediation, potentially reducing the effectiveness of mitigation systems, or impeding site investigations.

Although it is recognized that sorption may be used to treat indoor air contaminants, and passive sorption tube samplers are used prolifically in VI investigations, measuring contaminant sorption onto materials or soils is not a regular part of VI investigations and thus very little is known of the potential impact of this[3].

Over the years many VI sites have been investigated for their potential exposure risk. Most of these are conducted by private industries but a few notable academic ventures exist as well. Two well-known examples of these are the studies of "Sun Devil Manor" near Hill Air Force Base in Utah, and a building in Indianapolis, Indiana. Both of these sites were outfitted with a

wide variety of instrumentation to investigate the VI drivers at these sites. These studies yielded some of the richest VI datasets available and gave invaluable insights, in particular in the application of CPM[4] and sub-slab depressurization (SSD) mitigation systems[5, 6]. However, neither of these studies considered the role of sorption had at these sites.

The potential impact of sorption may perhaps be most significant in the application of the controlled pressure method and various mitigation schemes. The controlled pressure method (CPM) is the forced over- and depressurization of a building to max- and minimize the contaminant entry to the building. This aids the investigator to ascertain the worst-case VI scenario and help identify potential indoor contaminant sources[7, 4]. However, if the building has a large capacity to sorb contaminant vapors onto various materials, these may be sorbed and desorbed in response to the changing condition, potentially preventing corresponding changes in indoor air contaminant concentrations. The same is true for various mitigation schemes, while they may successfully prevent contaminant vapors from entering the house, these may still be released from the interior over an unknown period of time[1, 2].

1. building material adsorption were studied before, proved that adsorption is a thing

2. building material were studied most with other VOCs with relatively high concentration, which is rarely in the reality

3. TCE sorption of building materials at low concentration are less studied

In the past VI models have been used to gain insight into VI when no field or experimental data has been available. Previously examples of VI modeling studies are the role of rainfall in VI[8], or drivers of temporal variability in some of the aforementioned sites[9]. However, while many VI models include a sorption term in the governing equation for contaminant transport in soils, none have explored the role of sorption in VI. The reason for this is two-fold. First, there has been a general lack of interest in sorption and VI thus far. Secondly, the vast majority of VI modeling efforts and studies has focused on steady-state analyses of VI, and sorption only affects soil contaminant transport in time-dependent scenarios.

To bridge this knowledge gap we will begin to explore the role of sorption in VI through a combined effort of experimental and simulation work. Sorption data of TCE on various common indoor materials and Appalachian soil will be measured in a flow-chamber experiment. These sorption data will then be incorporated into a three-dimensional finite element model of

VI. For this purpose we will consider a prototypical VI scenario where a free-standing house with a basement is overlying a homogenously contaminated groundwater source. Using this model we will investigate how the dynamic contaminant transport is affected in general by sorption, how indoor sorption materials affect indoor air concentration as the building's pressurization fluctuates and how indoor air concentration are affected by indoor materials following successful mitigation of the structure.

## 2. Methods

### 2.1. Experimental Setup

The TCE dynamic sorption process of different building materials were determined by use of a method schematically shown in Figure 1. This method involved a selected material contained in an adsorption column through which TCE-containing gas was passed, and subsequent thermal desorption and measurement of the total amount of adsorption. During the adsorption part of the process, stainless steel tubes were packed with building materials held in place by glass wool. The amount of building material normally held in the tube was around 1 g. It was determined that neither the glass wool nor the stainless steel tube would retain significant amounts of TCE. The sample-containing tubes were first exposed desired low concentrations of TCE in nitrogen, which were then allowed to interact with the flow for varying periods of time. The typical flow rate of the nitrogen was 60 ml/min and the concentrations of TCE was around 1.1 ppbv. All of these adsorption experiments were conducted at room temperature. After a given time of exposure to the TCE-containing flow, that flow was stopped, and the sample tube was attached to a sorbent tube placed downstream of the sample tube. The sample tube was arranged such that the direction of the nitrogen flow in the subsequent desorption process was opposite that of the TCE-containing nitrogen flow during the adsorption process. During the thermal desorption step, the sample containing tube was covered by a heating mantle which permitted its heating at 100 °C. This allowed fully desorbing the TCE which had been held on the sample into a pure nitrogen flow, which carried it to the room temperature downstream sorbent tube, where it was again fully adsorbed. These tubes fully capture all of the TCE desorbed, from the samples, and the amount of TCE was analyzed by Gas Chromatography (GC) with an Electron Capture Detector(ECD).

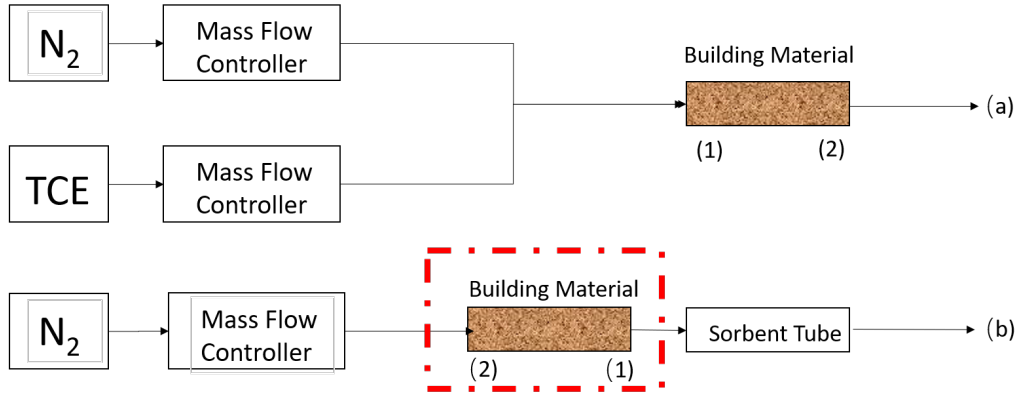


Figure 1: Schematic of experimental setup.

## 2.2. Numerical Model

To investigate the role of sorption in VI, we consider a simple VI scenario. Here we consider a house with a 10 by 10 m footprint, with the foundation bottom located 1 m below ground surface (bgs). The sole contaminant source is an uniformly TCE contaminated groundwater located 4 bgs, and the soil surrounding the house is assumed to homogenous and of a singular type. All contaminant vapors are assumed to enter the house through breaches in the foundation, modeled as a 1 cm wide crack that runs along the perimeter of the house. Finally we assume that sorption processes can occur both in the soil matrix and in the indoor environment (on various indoor materials).

Modeling this scenario requires us to simulate a couple of physics, many of which depend and interact with each other. The governing equations and the physics they govern are:

1. van Genuchten retention model - soil moisture.
2. Darcy's Law - air flow in the porous media.
3. Transport equation - contaminant transport in porous media.
4. Continuously stirred tank reactor (CSTR) - contaminant concentration in the indoor environment.

These physics are implemented in COMSOL Multiphysics, a commercial finite-element method package, which is used to solve our model. It is important to note that the indoor environment is implicitly modeled, but instead only given by the CSTR equation; the soil domain is explicitly modeled.

Figure 2: The vapor intrusion model

### 125 2.2.1. Vadose Zone Moisture Content

126 Since the contaminant transport occurs through three-phased the vadose  
 127 zone, it is important that we correctly account for soil moisture content and  
 128 its effect on advective and diffusive transport. In this modeled scenario, we  
 129 assume that the soil moisture is at steady-state and does not change, and  
 130 thus the soil moisture content is given by the retention model developed by  
 131 van Genuchten.

The van Genuchten retention model gives the soil water saturation as a function of elevation above groundwater. In turn this gives the water and gas filled porosities, and the relative permeability of the soil matrix.

$$Se = \begin{cases} \frac{1}{(1+\alpha z^n)^m} & z < 0 \\ 1 & z \geq 0 \end{cases} \quad (1)$$

$$\theta_w = \begin{cases} \theta_r + Se(\theta_s - \theta_r) & z < 0 \\ \theta_s & z \geq 0 \end{cases} \quad (2)$$

$$k_r = \begin{cases} Se^l [1 - (1 - Se^{\frac{1}{m}})]^2 & z < 0 \\ 0 & z \geq 0 \end{cases} \quad (3)$$

132 Se is the saturation, and ranges from 0 to 1, which represent completely un-  
 133 to fully saturated;  $z$  is the elevation above the groundwater in meters;  $\theta_r$ ,  
 134  $\theta_s$ ,  $\theta_w$ , and  $\theta_g$  are the residual moisture content, saturated porosity (or just  
 135 porosity), and water and air filled porosities respectively. All units are in  
 136 volume of phase divided by the volume of soil;  $k_r$  is the relative permeability  
 137 of water, which modifies the saturated permeability. This too ranges from 0  
 138 to 1, indicating completely im- and permeable respectively.  $1 - k_r$  gives the  
 139 relative permeability of air.

### 140 2.2.2. Gas Flow In The Vadose Zone

141 The gas flow in the vadose zone is governed by a modified version of  
 142 Darcy's Law. Originally, Darcy's Law was developed to describe flow in  
 143 saturated porous media, but since we're interested in flow in unsaturated  
 144 media, modification is necessary. An effective permeability that depends  
 145 on the relative permeability from van Genuchten is introduced to allow for  
 146 correct flow profiles in unsaturated porous media.

147 The vapor flow governing equation is given by

$$\frac{\partial}{\partial t}(\rho\theta_s) + \nabla \cdot \rho \left( - \frac{(1 - k_r)\kappa}{\mu} \nabla p \right) = 0 \quad (4)$$

148 Here  $\rho$  is the fluid density;  $\nabla$  is the del operator;  $\kappa$  is the saturated per-  
 149 meability;  $\mu$  is the fluid viscosity; and  $p$  is the fluid pressure. We assume  
 150 that the contaminant vapors are so dilute that the gas flow properties can  
 151 be taken to be those of air, and specifically at 20 °C and all the transport  
 152 properties may be found in Table 1.

*Boundary Conditions.* To solve (4) we assign the atmosphere boundary (see Figure 2) to be at reference pressure and act as a gauge, i.e. zero pressure. The foundation crack boundary is assigned the indoor-outdoor pressure difference value. Remaining boundaries are no-flow boundary conditions.

$$\text{Atmosphere} \quad p = 0 \text{ (Pa)} \quad (5)$$

$$\text{Foundation crack} \quad p = p_{\text{in/out}} \text{ (Pa)} \quad (6)$$

$$\text{All other} \quad -\vec{n} \cdot \rho_{\text{air}} \vec{u} = 0 \text{ (kg/(m}^2 \cdot \text{s))} \quad (7)$$

153 Here  $\vec{n}$  and  $\vec{u}$  are the boundary normal and gas velocity vectors.

154 *Initial Conditions.* For steady-state problems, the initial conditions don't  
 155 matter, but is simply zero for the entire domain. When solving transient,  
 156 the initial conditions are given by the steady-state solution.

### 157 2.2.3. Mass Transport In The Vadose Zone

158 Contaminants in the vadose zone exist in three phases - gaseous, solved in  
 159 water, and sorbed onto soil particles. While there are three distinct phases,  
 160 the water and gas phases are related via Henry's Law (8).

$$c_g = K_H c_w \quad (8)$$

161 Where  $c_g$  and  $c_w$  are the gas and water phase concentrations respectively in  
 162 mol/m<sup>3</sup>;  $K_H$  is the dimensionless Henry's Law constant.

163 In this work, we consider sorption between the soil and vapor phases, as  
 164 a function of the water contaminant concentration, through linear sorption  
 165 (9).

$$c_s = K_{\text{ads}} \rho_b c_g = K_{\text{ads}} \frac{\rho}{1 - \theta_t} K_H c_w \quad (9)$$

166 Here the  $c_s$  is the solid phase concentration in mol/kg;  $\rho_b$  is the bulk density  
 167 of the soil kg/m<sup>3</sup>, which is given by the density  $\rho$  and the total soil porosity  
 168  $\theta_t$ ;  $K_{\text{ads}}$  is the sorption isotherm in m<sup>3</sup>/kg. Using Henry's Law and the linear  
 169 isotherm we can express the total contaminant concentration in terms of the  
 170 water contaminant concentration.

171 Mass transport in the vadose zone is governed by diffusion and advection  
 172 and is given by (10).

$$R \frac{\partial c}{\partial t} = \nabla \cdot [D_{\text{eff}} \nabla c] - K_H \vec{u} \cdot \nabla c \quad (10)$$

173 The first term in (10) gives the change in contaminant water concentration  
 174 with respect to time, modified by the *retardation factor*,  $R$ , which is discussed  
 175 below; The second is the effective diffusive flux which is modified by the  
 176 effective diffusion coefficient  $D_{\text{eff}}$  which is also discussed below. The third is  
 177 the advective flux where  $\vec{u}$  is the soil-gas velocity from Darcy's Law, which  
 178 when multiplied with  $K_H$  gives the gas phase concentration advective flux.

179 *Contaminant entry into the building.* The contaminant enters the building  
 180 through a combination of advection and diffusive fluxes and is given by (11).

$$j_{ck} = \begin{cases} u_{ck} c_g - \frac{D_{\text{air}}}{L_{\text{slab}}} (c_{in} - c_g) & u_{ck} \geq 0 \\ u_{ck} c_{in} - \frac{D_{\text{air}}}{L_{\text{slab}}} (c_{in} - c_g) & u_{ck} < 0 \end{cases} \quad (11)$$

181 Here the  $j_{ck}$  is the molar contaminant flux into the building in mol/(m<sup>2</sup> · s);  
 182  $D_{\text{air}}$  is the contaminant diffusion coefficient in pure air in m<sup>2</sup>/s;  $L_{\text{slab}}$  is the  
 183 thickness of the foundation slab in m. The flux expression changes if there  
 184 is a bulk flow into the building, i.e.  $u_{ck} \geq 0$ , or out of the building.

185 *Retardation factor.* As the contaminants are transported through the vadose  
 186 zone, the partitioning between the various phases increases the contaminant  
 187 residency time, retarding the transport of contaminants. This effect is rep-  
 188 resented by  $R$  which is the retardation factor (12).

$$R = \theta_w + \theta_g K_H + \rho_b K_H K_{\text{ads}} \quad (12)$$

Here  $\theta_w$ ,  $\theta_g$  are the water and gas filled soil porosities;  $K_{\text{ads}}$  is the solid-gas  
 phase sorption isotherm in m<sup>3</sup>/kg. The diffusive and advective transport

retardation is proportional to the inverse of  $R$ .

$$D_{\text{retarded}} = \frac{D_{\text{eff}}}{R} \quad (13)$$

$$\vec{u}_{\text{retarded}} = \frac{\vec{u}}{R} \quad (14)$$

189 It should be noted that the soil-gas velocity,  $\vec{u}$ , is not retarded in of itself,  
190 but rather just the contaminant being transported through advection, giving  
191 a effective bulk velocity.

192 *Effective diffusivity.* The effective diffusivity in the vadose zone varies with  
193 the soil moisture content, from being close to that in water when fully sat-  
194 urated and vice versa. Millington-Quirk developed (15) which describes the  
195 effective diffusivity in variably saturated porous media.

$$D_{\text{eff}} = D_{\text{water}} \frac{\theta_w^{\frac{7}{3}}}{\theta_t^2} + \frac{D_{\text{air}}}{K_H} \frac{\theta_g^{\frac{7}{3}}}{\theta_t^2} \quad (15)$$

196 Where the porosity fractions are the water and gas phase tortuosity terms;  
197  $D_{\text{air}}$  and  $D_{\text{water}}$  are the contaminant diffusion coefficient in air and water  
198 respectively in  $\text{m}^2/\text{s}$ .

*Boundary Conditions.* A few boundary conditions are required to solve (10). In this model, the sole contaminant source is assumed to be the homogenously contaminated groundwater, which we assume to have a fixed concentration. The atmosphere acts as a contaminant sink, and any contaminant that makes it to this boundary is infinitely diluted, thus this is simply a zero concentration boundary condition. Contaminants leave the soil domain and enter the building through a combination of advective and diffusive gas phase transport. The last boundary condition is applied to all other boundaries and is a no-flow boundary.

$$\text{Groundwater} \quad c_w = 0 \text{ (mol/m}^3\text{)} \quad (16)$$

$$\text{Atmosphere} \quad c_w = c_{gw} \text{ (mol/m}^3\text{)} \quad (17)$$

$$\text{Foundation crack} \quad -\vec{n} \cdot \vec{N} = -\frac{j_{ck}}{K_H} \text{ (mol/(m}^2 \cdot \text{s))} \quad (18)$$

$$\text{All other} \quad -\vec{n} \cdot \vec{N} = 0 \text{ (mol/(m}^2 \cdot \text{s))} \quad (19)$$



199  $\vec{n} \cdot \vec{N}$  is the dot product between the boundary normal vector and the contam-  
 200 inant flux;  $j_c k$  is the contaminant vapor flux into the building. We assume  
 201 that only contaminants in the gas phase enter the building, and dividing  $j_{ck}$   
 202 by  $K_H$  we get proper accounting in terms of the water phase concentration.

203 *Initial Conditions.* For a steady-state condition the initial conditions don't  
 204 matter, but are set to be zero everywhere. For transient simulations in this  
 205 work, the steady-state solution is always used as an initial condition.

#### 206 2.2.4. Indoor Environment

207 The indoor air space is modeled as a continuously stirred tank reactor  
 208 (CSTR) given by (20). Contaminants are assumed to only enter through the  
 209 foundation crack, represented by  $n_{ck}$ , which is calculated by integrating the  
 210 contaminant flux over the foundation crack boundary. The product of air  
 211 exchange rate, which govern how many house volumes are exchanged with  
 212 the outside per time unit, and indoor air contaminant concentration gives the  
 213 contaminant exit rate. The sorption of contaminant is given by the sorption  
 214 reaction term in (22) and the sorbed contaminant concentration is given by  
 215 (21).

$$V_{\text{bldg}} \frac{\partial c_{\text{in}}}{\partial t} = n_{\text{ck}} - A_e c_{\text{in}} V_{\text{bldg}} + r_{\text{sorb}} V_{\text{mat}} \quad (20)$$

$$V_{\text{mat}} \frac{\partial c_{\text{sorb}}}{\partial t} = -r_{\text{sorb}} V_{\text{mat}} \quad (21)$$

$$r_{\text{sorb}} = k_1 c_{\text{sorb}} - k_2 c_{\text{in}} \quad (22)$$

$$n_{\text{ck}} = \int_{A_{ck}} j_c k dA \quad (23)$$

216 Here  $V_{\text{bldg}}$  and  $V_{\text{mat}}$  are the indoor control volume and volume of indoor  
 217 material in  $\text{m}^3$ ;  $c_{\text{in}}$  and  $c_{\text{sorb}}$  are the indoor and sorbed (onto the indoor mate-  
 218 rial) contaminant concentrations in  $\text{mol}/\text{m}^3$ ;  $n_{\text{entry}}$  is the contaminant entry  
 219 rate in  $\text{mol}/\text{s}$ ;  $r_{\text{sorb}}$  sorption rate in  $\text{mol}/(\text{m}^3 \cdot \text{s})$ ;  $k_1$  and  $k_2$  are desorption  
 220 and sorption reaction constants in  $1/\text{s}$ .

221 *Fitting Kinetic Parameters.* To calculate the indoor sorption rate we need  $k_1$   
 222 and  $k_2$ . These values are found by solving (22) numerically and then finding  
 223 the best  $k_1$  and  $k_2$  by fitting them to the experimental data via least square.  
 224 We use Runge-Kutta method of order 5(4) as the numerical solve, which

Table 1: Transport properties and model parameters

is implemented together with the least square method in the SciPy python package[10].

### 3. Results & Discussion

#### 3.1. Fitting Sorption Parameters

Using the numerical fitting scheme described in section 2.2.4 with the sorption data from the method described in section 2.1, the kinetic sorption parameters  $k_1$  and  $k_2$  are fitted. Figure 3 shows the result of this fitting and the sorption data for three select materials - wood, Appling soil, and cinderblock concrete. The  $k_1$  and  $k_2$  represent the rate at which TCE desorbs and sorbs respectively onto/from the material of interest. The equilibrium sorption constant is, using the formulation in (22), given by

$$K = \frac{k_1}{k_2} \quad (24)$$

and is used as the sorption isotherm. Here a small  $K$  indicate that there is a greater propensity for contaminant sorption.

To use the soil sorption isotherm in (10)  $K$  needs to be converted from being unitless to  $\text{m}^3/\text{kg}$ . This is done by multiplying the inverse of  $K$  isotherm with inverse of the soil bulk density  $\rho_b$ , which is taken to be  $1460 \text{ kg}/\text{m}^3$ .

$$K_{\text{ads}} = \frac{1}{K\rho_b} = 5.28 \text{ (m}^3/\text{kg)} \quad (25)$$

Table 2 shows the fitted parameters for the tested materials. Based on this these results we can see that cinderblock and soil have orders of magnitude larger sorption capacities than wood or drywall does. We can also see by the  $k_2$  values that soil and cinderblock sorb quickly, much faster than a material with similar sorptive capacity such as paper.

#### 3.2. Soil Sorption Retardation Effect

Building pressurization is a key factor in VI that influences the advective contaminant transport. The magnitude of change in response to a pressurization change is significantly influenced by a range of factors, such as soil

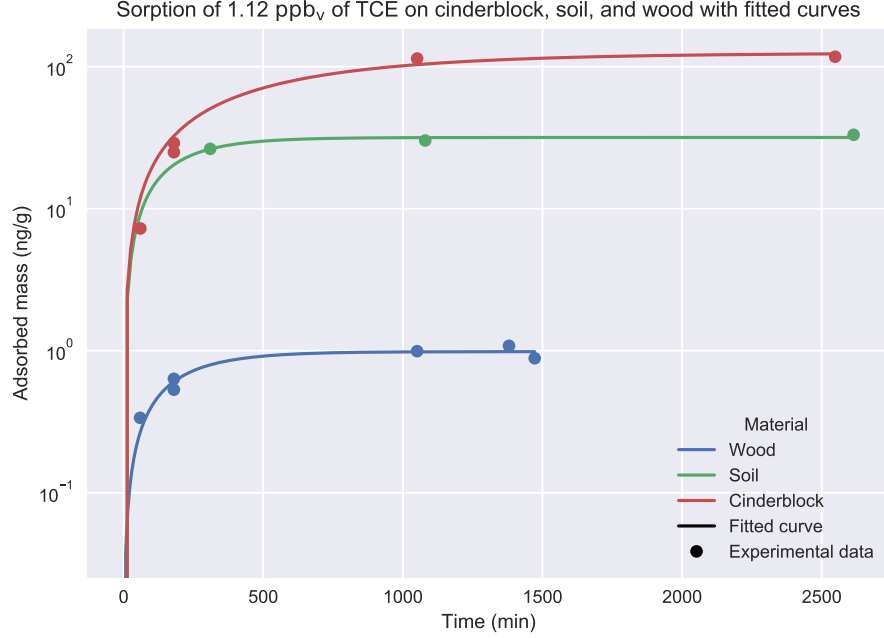


Figure 3: Experimental data of sorption of TCE onto three select materials as well as fitted sorption rates based on the kinetic model (22).

Table 2: Fitted kinetic sorption parameters based on sorption experiment data.

Material	$k_1$ (1/hr)	$k_2$ (1/hr)	$K$
Wood	0.32	44.90	$7.10 \cdot 10^{-3}$
Drywall	0.41	87.94	$4.65 \cdot 10^{-3}$
Carpet	0.26	58.74	$4.42 \cdot 10^{-3}$
Paper	0.04	88.37	$4.55 \cdot 10^{-4}$
Soil	0.34	2636.57	$1.30 \cdot 10^{-4}$
Cinderblock	0.10	4175.16	$2.40 \cdot 10^{-5}$

permeability, foundation depth, or soil moisture. To demonstrate the effect that soil sorption has on contaminant soil mass transport in the VI context, we run two types transient simulation where initially the modeled structure is at a steady -5 Pa, i.e. slightly depressurized. At the start of the simulation, the building building is 1) further depressurized to -15 Pa, or 2)

overpressurized to 15 Pa, and the simulation is allowed to run for 72 hours.

$$\text{Depressurization : } \Delta p_{\text{in/out}} = \begin{cases} -5, & t = 0 \text{ (hr)} \\ -15, & 0 < t \leq 72 \text{ (hr)} \end{cases} \quad (26)$$

$$\text{Overpressurization : } \Delta p_{\text{in/out}} = \begin{cases} -5, & t = 0 \text{ (hr)} \\ 15, & 0 < t \leq 72 \text{ (hr)} \end{cases} \quad (27)$$

For each of these cases, the simulation is run using two different soil types - sand and sandy loam. Sand is assumed here to not sorb any TCE, while for sandy loam a range of sorption isotherms are used. These range from no sorption to the experimentally determined sorption isotherm.

## 4. Conclusions

## Acknowledgements

This project was supported by grant ES-201502 from the Strategic Environmental Research and Development Program and Environmental Security Technology Certification Program (SERDP-ESTCP).

Declaration of interest: none

## References

- [1] R. Meininghaus, L. Gunnarsen, H. N. Knudsen, Diffusion and Sorption of Volatile Organic Compounds in Building Materials-Impact on Indoor Air Quality, *Environ. Sci. Technol.* 34 (15) (2000) 3101–3108. doi:10.1021/es991291i.
- [2] R. Meininghaus, E. Uhde, Diffusion studies of VOC mixtures in a building material, *Indoor Air* 12 (4) (2002) 215–222. doi:10.1034/j.1600-0668.2002.01131.x.
- [3] U.S. Environmental Protection Agency, OSWER Technical Guide for Assessing and Mitigating the Vapor Intrusion Pathway From Subsurface Vapor Sources To Indoor Air (2015).
- [4] C. Holton, Y. Guo, H. Luo, P. Dahlen, K. Gorder, E. Dettenmaier, P. C. Johnson, Long-Term Evaluation of the Controlled Pressure Method for Assessment of the Vapor Intrusion Pathway, *Environ. Sci. Technol.* 49 (4) (2015) 2091–2098. doi:10/f64j45.

- 272 [5] C. C. Lutes, R. S. Truesdale, B. W. Cosky, J. H. Zimmerman,  
273 B. A. Schumacher, Comparing Vapor Intrusion Mitigation System  
274 Performance for VOCs and Radon, *Remediation* 25 (4) (2015) 7–26.  
275 doi:10/gd6dfn.
- 276 [6] U.S. Environmental Protection Agency, Assessment of Mitigation Sys-  
277 tems on Vapor Intrusion: Temporal Trends, Attenuation Factors, and  
278 Contaminant Migration Routes under Mitigated And Non-mitigated  
279 Conditions (2015).
- 280 [7] T. McHugh, P. Loll, B. Eklund, Recent advances in vapor intrusion  
281 site investigations, *Journal of Environmental Management* 204 (2017)  
282 783–792. doi:10/gd6dgk.
- 283 [8] R. Shen, K. G. Pennell, E. M. Suuberg, A numerical investigation of  
284 vapor intrusion — The dynamic response of contaminant vapors to  
285 rainfall events, *Science of The Total Environment* 437 (2012) 110–120.  
286 doi:10/f4fp9s.
- 287 [9] J. G. V. Ström, Y. Guo, Y. Yao, E. M. Suuberg, Factors affect-  
288 ing temporal variations in vapor intrusion-induced indoor air contam-  
289 inant concentrations, *Building and Environment* 161 (2019) 106196.  
290 doi:10.1016/j.buildenv.2019.106196.
- 291 [10] E. Jones, T. Oliphant, Pearu Peterson, *SciPy: Open source scientific*  
292 *tools for Python* (2011).